Materials Today Bio 5 (2020) 100039

Contents lists available at ScienceDirect

Materials Today Bio

journal homepage: www.journals.elsevier.com/materials-today-bio

The molecular structure and multifunctionality of the cryptic plant polymer suberin

V.G. Correia [a], A. Bento [a,1], J. Pais [a,1], R. Rodrigues [a,1], Ł.P. Haliński [b], M. Frydrych [c], A. Greenhalgh [c], P. Stepnowski [b], F. Vollrath [c], A.W.T. King [d], C. Silva Pereira [a,*]

[a] Instituto de Tecnologia Química e Biológica António Xavier, Universidade Nova de Lisboa (ITQB NOVA), Av. da República, 2780-157, Oeiras, Portugal
[b] Department of Environmental Analysis, Faculty of Chemistry, University of Gdańsk, Wita Stwosza 63, 80-308, Gdańsk, Poland
[c] Department of Zoology, University of Oxford, Zoology Research and Administration Building, 11a Mansfield Road, Oxford, OX1 3SZ, United Kingdom
[d] Laboratory of Organic Chemistry, Department of Chemistry, University of Helsinki, A.I. Virtasen Aukio 1 (Chemicum), PL 55, 00014, Finland

ARTICLE INFO

Keywords:
Antimicrobial biopolymers
Solution-state nuclear magnetic resonance
Plant polyesters
Suberin particles
Polymer self-assembly
Suberin
Cryogenic milling of plant polymers

ABSTRACT

Suberin, a plant polyester, consists of polyfunctional long-chain fatty acids and glycerol and is an intriguing candidate as a novel antimicrobial material. We purified suberin from cork using ionic-liquid catalysis during which the glycerol bonds that ensure the polymeric nature of suberin remained intact or were only partially cleaved—yielding the closest to a native configuration reported to date.

The chemistry of suberin, both *in situ* (in cryogenically ground cork) and *ex situ* (ionic-liquid extracted), was elucidated using high-resolution one- and two-dimensional solution-state NMR analyses. Centrifugation was used to isolate suberin particles of distinct densities and their monomeric composition, assembly, and bactericidal effect, *inter alia*, were assessed.

Analysis of the molecular structure of suberin revealed the relative abundance of linear aliphatic *vs.* acylglycerol esters, comprising all acylglycerol configurations and the amounts of total carbonyls (C═O), free acid end groups (COOH), OH aliphatics, and OH aromatics. Suberin centrifuged fractions revealed generic physiochemical properties and monomeric composition and self-assemble into polygonal structures that display distinct degrees of compactness when lyophilized. Suberin particles—*suberinsomes*—display bactericidal activity against major human pathogenic bacteria.

Fingerprinting the multifunctionality of complex (plant) polyesters such as suberin allows for the identification of novel polymer assemblies with significant value-added properties.

1. Introduction

During the colonization of land by plants, *ca.* 450 million years ago, plants acquired the capacity to synthesize the related biopolymers, cutin and suberin [1,2]. Due to this evolutionary event, plants were able to add a defensive hydrophobic barrier to their cell walls [3–5]. Due to the advantages this conferred, these polyesters now constitute the fourth most abundant class of plant polymers, after cellulose, hemicellulose, and lignin. Plant polyesters can be regarded as evolutionarily optimized multifunctional biopolymers controlling many aspects of plant biology. Altered cutin and/or suberin structures result in divergent phenotypes, including: altered susceptibilities to both biotic and abiotic stresses; variable morphologies and altered permeabilities, among others [6].

Many studies have focused on suberin from cork as an archetypal plant polyester, as it accounts for *ca.* 30–50% of the mass of cork [7]. Suberin is a heterogeneous mixture of poorly understood and poorly characterized polymeric units. Suberin contains both linear alkyl and aromatic moieties of monomers linked through acylglycerol or linear aliphatic esters [3,5,8,9]. Consequently, extraction of suberin from plant sources requires ester cleavage, commonly achieved using non-specific hydrolyses that release monomeric and/or small oligomeric constituents [10,11]. The innovative use of ionic liquid-based catalysis to specifically cleave a limited number of acylglycerol esters enables the recovery of more complex, esterified suberin structures [12–16]. These structures can spontaneously rearrange *ex situ* into waterproof, bactericidal, and antibiofouling materials [16,17].

* Corresponding author.
E-mail address: spereira@itqb.unl.pt (C. Silva Pereira).
[1] Equal contributing authors.

https://doi.org/10.1016/j.mtbio.2019.100039
Received 30 September 2019; Received in revised form 13 December 2019; Accepted 16 December 2019
Available online 26 December 2019

To date, our understanding of the chemistry of cork suberin has been seriously hampered as current solution-state-based methods only allow for the analysis of the component monomers/small oligomers [11,18] while solid-state methods exhibit poor resolution in revealing the bulky chemical functionalities and properties of the complete polymer/larger oligomers [10,15,16]. Consequently, our current knowledge is not sufficient to demonstrate correlations between specific aspects of polymer chemistry and the resulting physical and biological properties.

Suberin assemblies of fatty acids and their acylglycerides are promising materials for a number of applications as they possess some very exciting properties, including generally a non-cytotoxic nature [19]. Another such property is suberin's ability to inhibit the growth of bacteria, and thus it constitutes a promising alternative with which to fight bacterial species in the post-antibiotic era [20]. Inspired by this, we strive to better understand the physical and chemical structure of suberin, and we have established a methodological approach with which to begin to unravel the chemistry and functionality of complex assemblies of this biopolymer. In particular, we have applied a suite of 1D- and 2D-solution-state NMR methods that is complemented by other morphological, physical, and biological assays. Despite the high complexity of the biopolymer backbone, here we successfully assign suberin's monomeric constituents by NMR, guided by complementary solution-state NMR analyses of cryogenically milled cork. Suberin assemblies of *ca.* 200–400 nm and of distinct compactness showed slight differences in their monomeric composition. These suberin assemblies showed antimicrobial activity against *Staphylococcus aureus* and *Escherichia coli*. We trust this methodological strategy will support the identification of complex polymers assemblies of interesting biological properties in the near future.

2. Materials and methods

2.1. Chemicals

All reagents were of high analytical grade and purchased from Sigma-Aldrich, except diethyl ether (Panreac, 99.7%), dimethylsulfoxide (DMSO, Fisher Chemical, 99.98%), and deuterated DMSO (DMSO-d_6, Merck, 99.8%). Cork was obtained from Amorim & Irmãos SA (Santa Maria de Lamas, Portugal) and processed as previously described [13].

2.2. Biological samples preparation

Suberin was extracted from cork using cholinium hexanoate [12] ($[N_{111}C_2H_4OH][O_2CC_5H_{11}]$, water content ~1.8%) as described before [13], (2 h, 100 °C, without stirring). After stopping the reaction by adding cold DMSO, the mixture was filtered (the insoluble residue recovered and washed) and suberin precipitated by adding water (4 °C) and recovered by centrifugation (4 °C, 1 h) at 2452 *g* for the parental sample or sequentially at 96, 385, 865, 1538, and 2452 *g* for the suberin centrifuged fractions. All samples were kept lyophilized (FreeZone 4.5 L −105 °C Benchtop Freeze Dryers, Labconco) under a controlled atmosphere until further use. Cork and cork residue were solubilized with the aid of cryogenic milling using a RESTCH Cryomill equipped with a 25 mL grinding jar with six zirconium oxide grinding balls (10 mm) (Supplementary Fig. S7).

2.3. Microscopic analyses

Transmission electron microscopy (TEM, Hitachi H-7650) was used to analyze suberin assemblies, and scanning electron microscopy (SEM, JEOL JSM-7001F) was used to analyze the lyophilized suberin samples.

2.4. Chemical characterization methods

Nuclear magnetic resonance (NMR) spectra were recorded using a UNITY INOVA 600 MHz (Varian Inc., Palo Alto, CA, USA) or an Avance II + 800 MHz (Bruker Biospin, Rheinstetten, Germany) spectrometers. All NMR spectra (^{1}H, ^{13}C, COSY, DOSY, HSQC, HMBC, TOCSY) were acquired in DMSO-d_6 using 5 mm diameter NMR tubes, at 60 °C as follows: 50 mg of purified suberin in 550 μL of DMSO-d_6 (^{1}H, ^{13}C, HSQC, HMBC and TOCSY), with the use of benzene as internal standard for quantitative approaches (Q-^{13}C spectra); 5 mg of suberin centrifuged fractions in 550 μL of DMSO-d_6 (^{1}H, HSQC, DOSY), and 50 mg of cryomilled cork/cork residue in 550 μL of DMSO-d_6 (^{1}H, HSQC). Quantitative ^{31}P NMR of suberin was also performed (Supplementary Fig. S10). MestReNova, Version 11.04–18998 (Mestrelab Research, S.L.) and TopSpin, Version 3.5 pl 7 were used to process the raw data acquired in the Varian and the Bruker spectrometers, respectively.

Gas chromatography–mass spectrometry (GC-MS). The hydrolyzable monomeric constituents of suberin samples (*ca.* 10 mg) were methylated and silylated (hexadecane added as internal standard) prior to quantification by GC-MS (Agilent: 7820A GC and 5977B quadrupole MS; HP-5MS column) operated as follows: 80 °C, 4 °C·min^{-1} until 310 °C; 310 °C during 15 min [10]. Data were acquired using a MSD ChemStation (Agilent); compounds identified based on EI-MS fragmentation patterns, including the Wiley-NIST reference library and previous published data [13,15], and quantified using external standards of the major classes of suberin aliphatic (hexadecanoic acid, hexadecanedioic acid, and pentadecanol) and aromatic monomers (cinnamic acid), at the limits of 5.2–104 μg and 50–1000 μg, respectively. All samples were analyzed in triplicates and also in technical duplicates for a few randomly selected samples.

Elemental analysis and liquid chromatography were used to quantify of C/H/N/S/O (see Supplementary Information) and glycerol [16], respectively.

2.5. Thermal analyses

Thermal gravimetric analyses (TGA) was performed using a Q500 (TA Instruments, USA), and differential scanning calorimetry (DSC) measurements were performed using a Q2000 (TA Instruments, USA) (see Supplementary Information).

2.6. Antimicrobial assays

S. aureus NCTC8325 and *E. coli* TOP 10 cells (5×10^5 cells·mL^{-1}) in Mueller-Hinton broth (MHB) media were exposed to suberin concentrations ranging from 0.25 to 2 μg mL^{-1} (11 h, 37 °C, without agitation). Suberin was added to the media from a stock solution in DMSO to a final concentration of 2% v/v. Cellular morphology and viability were visualized using light and fluorescence microscopy (with the fluorescent dye propidium iodide), respectively, with an inverted Zeiss Axio Observer microscope equipped with a Photometrics CoolSNAP HQ2 camera (Roper Scientific). Controls of the medium, bacterial growth, and hydrolysate cork monomers (obtained by alkaline hydrolysis) were also carried out. Under the same conditions, the average hydrodynamic diameter (dh), the dispersity (PDI), and the zeta potential (Zp) of each sample were measured using dynamic light scattering (DLS) analysis (triplicates; each in technical triplicate) (see Supplementary Information).

2.7. Availability of data and material

Supplementary Information word document is available, containing more detailed tables and figures that support the figure panels in the main text.

3. Results and discussion

Suberin was isolated from cork via mild cleavage of acylglycerol esters catalyzed by cholinium hexanoate [16]. During the course of this reaction, oligomers are continuously released from the cork cell walls [16], possibly increasing the dispersity of the isolated suberin. Here, in order to reduce dispersity, the cleavage of acylglycerol esters was limited

by interrupting the reaction when half of the suberin present in cork had been extracted. The purified suberin precipitated in water where it spontaneously self-assembled into asymmetrical assemblies of various sizes on the microscale as observed by TEM imaging (Fig. 1a). Following lyophilization, suberin was observed by SEM to be composed of ordered, elongated polygon structures, with polygonal facets of thousands of μm^2 and with lengths ranging from 100 to 175 μm (Fig. 1b). The preservation of the majority of the biopolymer backbone was apparent as the purified suberin contained 39.12 mg of glycerol *per* g (Table 1). This value is very close to that estimated for glycerol in cork following removal of non-covalent constituents that have been previously reported (*ca.* 4–5% w/w) [21,22]. The elemental composition of our purified suberin consisted of: 64.07% C (±0.02), 8.86% H (±0.06), 26.08% O (±0.04), and 1.60% N (±0.08) (Supplementary Table S1). This is a *ca.* 4% increase in O content compared to previously characterized suberinic structures containing less than *ca.* 13% of native glycerol [13,16]. Thermal characterization of suberin via TGA and DSC demonstrated temperature decomposition profiles with a gradual, multistep weight loss and a broad melting curve that was consistent over the entire range of isolated fractions (Supplementary Fig. S1). The near-native crosslinked arrangement of suberin is reflected in its high thermal decomposition point (to ~382 °C) similar to that reported before (~368 °C) [15].

Many studies have relied on solution-state NMR-based methods to reveal the chemistry of suberinic materials [10,23,24]. However, these studies have only focused on the soluble monomers and/or small oligomers. Here we attained, for the first time, a wide-ranging NMR characterization of crosslinked suberin structures upon their solubilization in DMSO at 80 °C (Fig. 2, Supplementary Table S2 and Fig. S2-4). The assignment of ^{1}H and ^{13}C chemical shifts for the constituent monomers was achieved through a combination of $^{1}H–^{1}H$ (COSY) and $^{1}H–^{13}C$ (HSQC, HMBC) correlation experiments. The collected spectra showed many overlapping signals; an archetypal feature observed in other complex multifunctional polymers [25]. As an illustration, the ^{1}H and ^{13}C spectra of suberin, as well as the full range HSQC spectrum, are depicted in Fig. 2(a–c). Highlighted are the regions corresponding to aliphatics (d), CH/CH_2-X aliphatics and glycerol CH-acyl (e), and aromatics (f). The relative abundances of aliphatics, CH/CH_2-X aliphatics, glycerol CH-acyl, and aromatics were estimated, through the integration of the ^{1}H-spectrum, as: 67%, 28%, 3% and 2%, respectively. The aliphatic nature of the biopolymer was also highlighted by the GC-MS data on its hydrolysate constituents (*i.e.,* those released upon alkaline hydrolysis). The hydrolysate constituents accounted for 43.0 ± 2.7% (w/w) of total mass with an identification yield of ~35% (w/w) (Table 1, Supplementary Fig. S5). The limits on the identification yield by GC-MS are usually attributed to

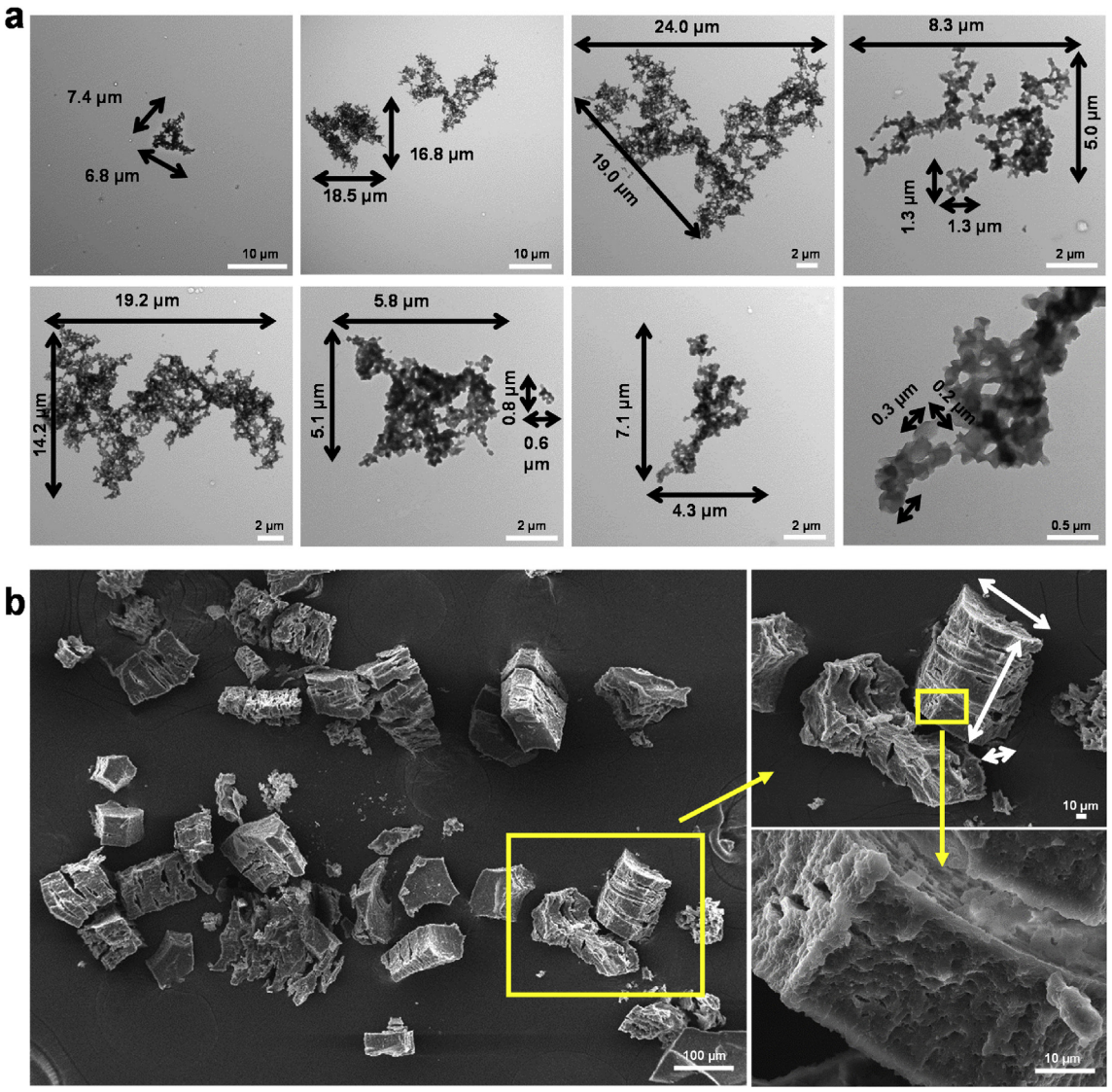

Fig. 1. Microscopy imaging of the purified suberin. (a) Suberin in water formed aggregates of various sizes on the μm scale as observed by TEM imaging. (b) Corresponding freeze-dried samples formed ordered polygonal structures as observed by SEM imaging.

Table 1

Quantitative analysis of the monomeric hydrolysable constituents of suberin. GC-MS was used to quantify the hydrolysable monomers of purified suberin (parental sample) and of its composing centrifuged fractions. Results are given as mg of compound *per* gram of dried starting material. The identification yields (wt %) are indicated below. The glycerol released upon alkaline hydrolysis of the samples and quantified by HPLC is also indicated. Different letters distinguish statistical differences ($p < 0.05$) between suberin samples ($n = 3$), assessed by pairwise t-tests comparisons. All the analyses were performed using the XL-STAT software version 2014.1.02 (Addinsoft).

GC-MS	$m_x/m_{suberin}$ (mg/g)			
Compound	Suberin	Suberin fraction 96 *g*	Suberin fraction 385 *g*	Suberin fraction 865 *g*
Alkan-1-ols [2.2–3.3% wt]	**11.74 ± 0.43**	**10.45 ± 0.61**	**7.97 ± 1.29**	**7.02 ± 1.24**
hexadecan-1-ol	0.15 ± 0.05	0.09 ± 0.01	0.12 ± 0.03	0.12 ± 0.01
octadecan-1-ol	1.27 ± 0.37	1.21 ± 0.67	0.92 ± 0.41	0.87 ± 0.26
eicosan-1-ol	0.82 ± 0.22	0.63 ± 0.13	0.66 ± 0.16	0.62 ± 0.18
docosan-1-ol	2.07 ± 0.36	1.77 ± 0.28	1.72 ± 0.14	1.63 ± 0.31
tetracosan-1-ol*	7.44 ± 0.63[a]	6.75 ± 1.09[a,b]	4.54 ± 1.02[b,c]	3.79 ± 1.03[c]
Alkanoic acids [3.3–3.9% wt]	**12.51 ± 1.67**	**11.19 ± 0.94**	**11.30 ± 0.85**	**12.69 ± 1.57**
tetradecanoic acid	0.53 ± 0.03[a]	0.51 ± 0.03[a]	0.59 ± 0.10[a,b]	0.70 ± 0.03[b]
hexadecanoic acid	1.19 ± 0.06[a,b]	1.26 ± 0.22[a,b]	1.42 ± 0.22[b,c]	1.69 ± 0.11[c]
9,12-octadecadienoic acid	0.43 ± 0.12	0.39 ± 0.11	0.38 ± 0.09	0.48 ± 0.11
9-octadecenoic acid	0.74 ± 0.19	0.66 ± 0.11	0.68 ± 0.10	0.68 ± 0.11
octadecanoic acid	1.11 ± 0.05	1.16 ± 0.22	1.17 ± 0.21	1.39 ± 0.17
eicosanoic acid	1.83 ± 0.38	1.64 ± 0.32	1.59 ± 0.31	1.64 ± 0.44
docosanoic acid	6.69 ± 1.12	5.58 ± 0.36	5.47 ± 0.20	6.12 ± 0.83
ω-Hydroxyalkanoic acids [45.4–46.7% wt]	**164.86 ± 6.62**	**158.70 ± 5.94**	**154.21 ± 4.09**	**146.35 ± 7.41**
16-hydroxyhexadecanoic acid	3.84 ± 0.35	3.41 ± 0.20	3.46 ± 0.18	3.40 ± 0.40
18-hydroxyoctadec-9-enoic acid	36.39 ± 1.54	36.11 ± 1.20	37.37 ± 1.39	38.61 ± 1.00
18-hydroxyoctadecanoic acid	0.94 ± 0.34	0.73 ± 0.31	0.86 ± 0.32	0.77 ± 0.37
20-hydroxyeicos-11-enoic acid	9.96 ± 1.00[a]	9.14 ± 0.37[a]	9.68 ± 0.33[a]	7.13 ± 0.91[b]
20-hydroxyeicosanoic acid	5.57 ± 0.80	4.94 ± 0.60	5.12 ± 0.42	5.01 ± 1.04
22-hydroxydocosanoic acid	57.95 ± 2.66	51.84 ± 2.91	53.87 ± 2.96	55.58 ± 3.32
24-hydroxytetracosanoic acid	17.84 ± 1.44[a]	14.22 ± 0.89[b]	14.56 ± 0.57[b]	10.01 ± 2.00[c]
8,18-dihydroxyoctadec-9-enoic acid	2.22 ± 0.49	1.48 ± 0.20	1.50 ± 0.25	1.27 ± 0.42
?,18-dihydroxyoctadec-9-enoic acid	1.71 ± 0.33	1.24 ± 0.20	1.23 ± 0.17	1.25 ± 0.37
?,?,?-trihydroxyoctadec-12-enoic acid	9.15 ± 1.00[a]	3.10 ± 0.59[b]	3.74 ± 0.58[b]	3.19 ± 0.29[b]
9,10,18-trihydroxyoctadecanoic acid	4.20 ± 1.10[a,b]	3.32 ± 0.37[b]	5.19 ± 0.98[a,c,d]	8.75 ± 2.42[d]
9,10-epoxy-18-hydroxyoctadecanoic acid*	15.08 ± 3.15[a]	29.18 ± 0.75[b]	17.63 ± 2.35[a]	11.38 ± 1.05[c]
α,ω-Alkanedioic acids [43.6–46.6% wt]	**154.18 ± 6.40**	**149.50 ± 7.95**	**149.48 ± 2.46**	**150.31 ± 3.29**
hexadecanedioic acid	11.57 ± 0.54[a]	10.38 ± 0.33[b]	9.93 ± 0.73[b]	10.64 ± 0.35[b]
octadec-9-enedioic acid	20.43 ± 0.99	21.23 ± 0.30	21.29 ± 0.60	21.12 ± 0.54
octadecanedioic acid	51.27 ± 2.12[a]	50.87 ± 1.70[a]	52.77 ± 2.11[a]	56.18 ± 0.62[b]
eicosanedioic acid	6.09 ± 0.58	5.64 ± 1.11	5.49 ± 0.37	6.36 ± 1.49
9,10-dihydroxyoctadecanedioic acid	36.00 ± 0.55[a]	32.03 ± 2.02[b]	32.96 ± 3.11[a,b,c]	29.18 ± 1.41[b,c]
docosanedioic acid	26.20 ± 2.12	27.78 ± 2.70	25.17 ± 3.14	24.66 ± 0.83
9,10-dihydroxyeicosanedioic acid	2.62 ± 0.99	1.56 ± 0.83	1.88 ± 0.911	2.18 ± 1.01
Phenolics [0.7–0.8% wt]	**2.55 ± 0.18**	**2.37 ± 0.06**	**2.21 ± 0.70**	**2.62 ± 0.17**
4-hydroxy-3-methoxy-cinnamic acid (ferulic acid)	2.31 ± 0.22	2.10 ± 0.05	1.96 ± 0.69	2.18 ± 0.16
4-hydroxy-3-methoxybenzoic acid (vanillic acid)	0.25 ± 0.05[a]	0.27 ± 0.01[a]	0.25 ± 0.02[a]	0.44 ± 0.01[b]
Extractives [0.8–2.0%]**	**7.13 ± 0.93**	**3.85 ± 0.73**	**4.33 ± 0.28**	**2.73 ± 1.47**
hexadecahydrocyclopentachrysen-9-ol (betuline)	4.70 ± 0.25[a]	2.81 ± 0.41[b]	3.24 ± 0.23[b]	1.64 ± 0.99[b]
hexadecahydrocyclopenta chrysene-3-carboxylic acid (betulinic acid)	2.43 ± 1.03	1.03 ± 0.32	1.08 ± 0.25	1.09 ± 0.48
Glycerol [~0.2% wt]	**0.57 ± 0.10**	**0.70 ± 0.11**	**0.57 ± 0.11**	**0.54 ± 0.08**
Identification Yield (wt%)	**35.35 ± 1.42**	**34.06 ± 1.59**	**31.84 ± 0.60**	**32.23 ± 1.48**
HPLC				
Glycerol	**38.55 ± 3.11[a]**	**44.11 ± 4.17[a,b]**	**44.30 ± 2.56[a,b]**	**45.44 ± 0.96[b]**

Total amount of glycerol is calculated by adding the values obtained by GC-MS and HPLC

Pairwise *t*-tests comparisons were used to identify significant differences between suberin samples ($p < 0.05$).

* Quantification influenced due to their coelution.

** Extractives are not considered suberin monomeric constituents.

non-volatile high-molecular-weight oligomeric structures [11]. Of the monomers identified, nearly 98% (w/w %) were aliphatic compounds with only a minor contribution from aromatic compounds (0.72 ± 0.06, w/w %). Specifically, we identified ω-hydroxyacids and α,ω-diacids in significant amounts. Fatty acids (alkanoic acids), fatty alcohols (alkanols), and aromatics were identified in low amounts. The level of glycerol detected by GC-MS was ~0.2% (w/w) since most of this hydrolysate monomer is lost in the aqueous phase prior to the analysis [26]. Due to improvement in the analytical methodology, some suberin constituents were identified for the first time, *viz.* hexadecan-1-ol and one trihydroxyoctadec-12-enoic acid isomer. Detection of similar levels of monomers carrying epoxy rings in both suberin and cork, by GC-MS (Supplementary Table S3), implied that cleavage of the epoxy ring is not favored by the ionic-liquid catalyzed hydrolysis. The hydrolysate constituents found in suberin were similar, both in diversity and in abundance (w/w %), to those identified in cork (Supplementary Table S3). In suberinic materials previously isolated using a similar method, yet containing *ca.* fivefold less glycerol compared to the suberin isolated for this study, the detected amount of alkanedioic acids was much lower [13]. Seemingly, retention of glycerol at (near) native levels in the suberin here purified reduced the release from the polymer backbone of oligomers/monomers rich in alkanedioic acids, which would be otherwise lost during subsequent processing.

To look "inside" the backbone of suberin, specifically at its cross-linking through acylglycerol bonds, we analyzed the presence and relative abundance of each acylglycerol configuration (Fig. 2e,g). We found that suberin contained all five possible configurations, similar to previous observations of suberin oligomers from potato peel, recovered using a

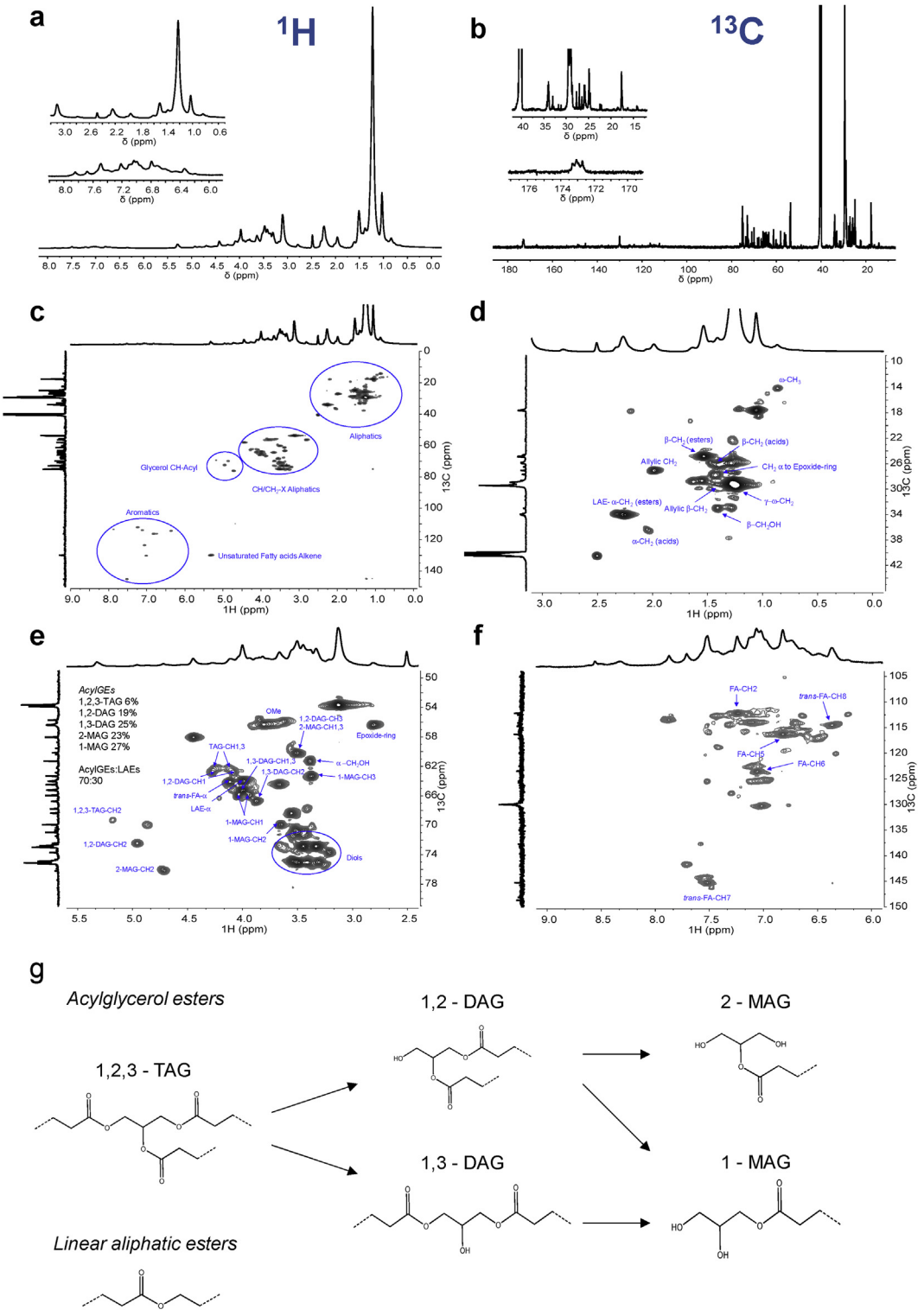

Fig. 2. Wide-ranging NMR spectral characterization of purified suberin. (a) The NMR ^{1}H and (b) ^{13}C spectra, with inserts focusing on the aliphatic and aromatic regions; and the HSQC spectrum: (c) full and regions corresponding to (d) aliphatics, (e) glycerol CH-Acyl and CH/CH_2-X aliphatics, and (f) aromatics of the purified suberin. (g) The chemical structure of linear aliphatic esters and of acylglycerol esters comprising all possible configurations are presented. Text inserts in the HSQC spectra indicate the relative abundance (%) of the different acylglycerol configurations present within each sample as well as the ratio of aliphatic esters and acylglycerol esters. AcylGEs and LAEs stand for acylglycerol esters and linear aliphatic esters, respectively; TAG, DAG, and MAG stand for triacylglycerol, diacylglycerol, and monoacylglycerol, respectively. Some correlations (unlabeled) are uncertain or unidentified.

non-specific partial hydrolysis [18]. To estimate the relative abundance of each acylglycerol configuration, we measured the contour volume integrals of the glycerol CH2 signals in the HSQC spectra (Fig. 2e, Supplementary Fig. S6). This integration method was proposed before for the elucidation of lignin subunit composition and lignin interunit linkage distribution [27,28]. Most of the retained glycerol was found in monoacylglycerol (MAG) or diacylglycerol (DAG) configurations: 50% and 44% of the total glycerol, respectively. Only 6% of retained glycerol

was found in the triacylglycerol configuration (1,2,3-TAG). Specifically, suberin contains *per* g: 10.6 mg of 1-MAG (27%), 9.0 mg of 2-MAG (23%), 9.8 mg of 1,3-DAG (25%), 7.4 mg of 1,2-DAG (19%), and only 2.3 mg of 1,2,3-TAG (6%).

To clarify if the di- and mono-acylglycerol configurations resulted from the partial hydrolysis of suberin, we also collected solution-state ^{1}H and HSQC spectra for cork (and for its residue after suberin removal by the ionic liquid), following cryogenic vibratory milling. This was the first time that a combined cryogenic milling and NMR method was applied to insoluble cork and was based on similar milling studies on wood, regardless that in previous studies ball milling was applied instead of cryogenic milling [29,30]. The optimized milling process efficiently fractured the cellular organization of the plant tissue as shown by SEM imaging (Fig. 3a, Supplementary Fig. S7). During the cryogenic milling, oxidation of cork may occur inside the grinding jar due to possible condensation of oxygen at low temperatures. Elemental analysis of cork before and after the milling process showed no differences in their relative percentage of oxygen (Supplementary Table S1). The ATR-FTIR spectra of cork before and after the milling process and of their corresponding insoluble residues (*i.e.,* after removal of suberin by the ionic liquid or after direct solubilization in DMSO) are also virtually identical (Supplementary Figure S8). Finally, the relative abundances of the hydrolysate constituents remain unaltered after the cryogenic milling (Supplementary Table S3 and S4), not showing any statistically relevant difference (Levene analysis, p-value = 0.40).

Suberin corresponds to nearly 50% and 25% of the weights of cork and of cork residue, respectively, hence the similarity of the chemical signatures found in the corresponding ^{1}H NMR spectra (Fig. 3b). The relative abundance of each glycerol configuration in suberin, assessed via HSQC peak volume integration, was compared to configurations found in cork (Fig. 3c) and in the corresponding cork residue after removal of suberin by the ionic liquid (Fig. 3d). The cork residue mirrored the acylglycerol configurations that were found in purified suberin, although in distinct proportions: 1,2,3-TAG, 1,3-DAG, 1,2-DAG, 1-MAG, and 2-MAG accounted for 26%, 27%, 18%, 18%, and 11% of the total glycerol, respectively. As expected, 1,2,3-TAG was found in cork but 1,2-DAG was also found in a significant proportion. 1,2,3-TAG and 1,2-DAG accounted for 69% and 31% of the total glycerol, respectively. This result is consistent with the conversion of 1,2-DAG to 1,2,3-TAG through the action of an acyl-CoA:diacylglycerol acyltransferase during suberin biosynthesis [6]. Hence, our methodological approach may open new means by which to monitor suberin biosynthesis and/or deposition *in planta*. Evidently, the extraction of suberin from cork by the ionic liquid proceeded through the preferential cleavage of acylglycerol esters bonds at the C2 position, as denoted by the increased ratio of 1,3-DAG to 1,2-DAG in the purified suberin, as proposed previously [16]. In addition, we also inferred the relative amounts of linear aliphatic esters and acylglycerol esters present in suberin, as *ca.* 30% and 70%, respectively (Fig. 2e, Supplementary Fig. S6), from their respective volume contour integrals in the HSQC spectrum [27]. The natural abundance of linear aliphatic esters in suberin *in situ* (*i.e.*, in the cryogenically milled cork) was estimated as *ca.* 40% of the total esters (similar to that estimated for the cork residue). Here, the contour volume integrals are obscured by many overlapping signals and thus 40% may reflect their over-representation (Supplementary Fig. S9). This result highlights that in the ionic liquid extracted biopolymer, at least 75% of the linear aliphatic

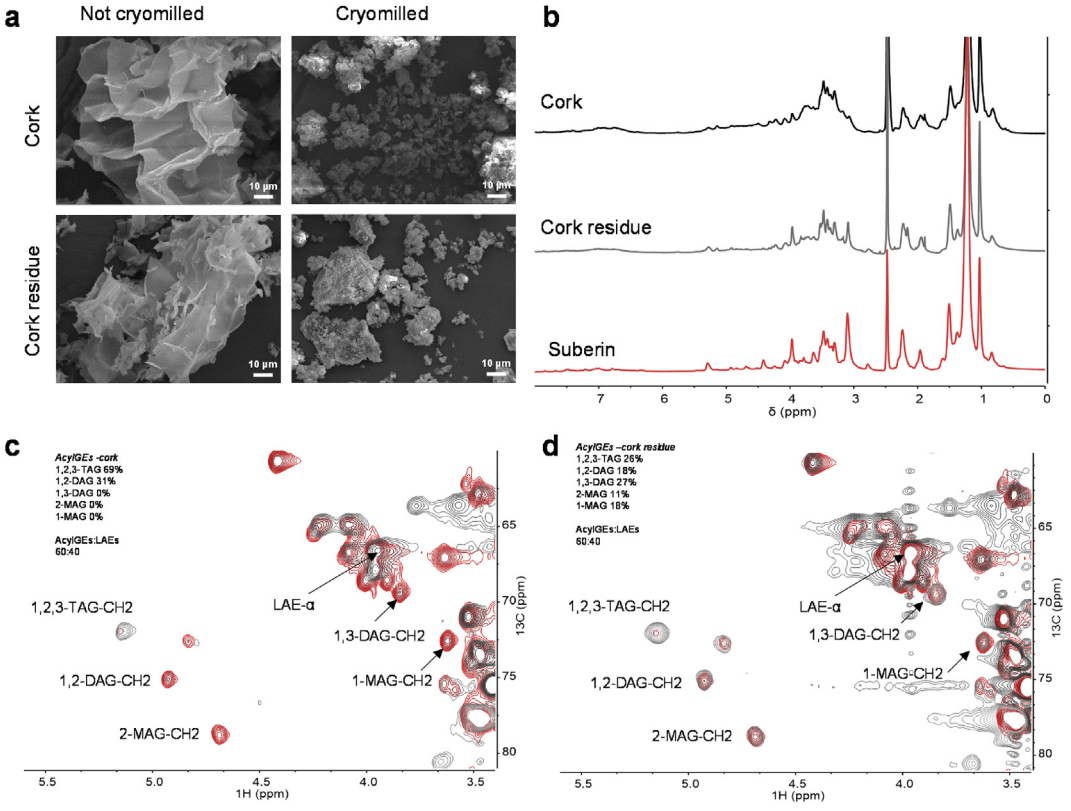

Fig. 3. Morphological and NMR chemical characterization of cryogenic milled cork and its residue after suberin removal. (a) Cryogenic milling was used to pulverize cork and its residue following suberin removal, (b–d) at levels that allow solubilization in heated DMSO for wide-ranging solution-state NMR spectral analyses. (a) SEM micrographs of cork and cork residues before and after cryomilling for 4 h show that the cork cell wall structure completely disappeared. (b) The ^{1}H NMR spectra of cork and cork residue show great chemical similarity to that of suberin. Comparison of the glycerol CH-Acyl region of the HSQC-NMR spectra of cork (c, gray) and of cork residues (d, gray) with that of suberin (c–d, red). Text inserts in the HSQC spectra indicate the relative abundance (%) of the different acylglycerol configurations present within each sample as well as the ratio of aliphatic esters and acylglycerol esters. AcylGEs and LAEs stand for acylglycerol esters and linear aliphatic esters, respectively; TAG, DAG, and MAG stand for triacylglycerol, diacylglycerol, and monoacylglycerol, respectively.

esters maintained their native configuration. The hydrolysate constituents identified in the ionic liquid purified suberin and the *in situ* suberin are comparable (Levene analysis, p-value = 0.54), regardless of a statistically relevant enrichment of the fatty acids family for the *in situ* suberin (one-way ANOVA, p-value<0.05). Fatty acids are end-chain monomers, hence prone to be lost due to ester cleavage catalyzed by the ionic liquid but preserved in the *in situ* suberin.

In the suberin polymer, we calculated that 20.5% of the total carbonyl groups (C═O) are free acid (COOH) end groups, corresponding to the amounts calculated through quantitative ^{13}C- and ^{31}P- NMR: 1.47 mmol g^{-1} and 0.30 mmol g^{-1}, respectively (Supplementary Fig. S10 and S11). The formation of free acids did not result from extensive cleavage of linear aliphatic esters (not favored in the conditions used), nor from the release of glycerol, the majority of which was retained in the biopolymer. Accordingly, we estimate that acylglycerol esters account for *ca.* 44% of the total carboniles (0.66 mmol g^{-1} of suberin; weight of their relative molar contributions and the number of moles of carboniles in each configuration), whereas linear aliphatic esters account for *ca.* 36% (0.52 mmol·$g^{-1}$of suberin) close to the 30% estimated earlier (Fig. 2e). Any direct quantification of naturally occurring free acids in suberin is obscured by the presence of lignin in cork [31]. From the quantitative ^{31}P spectrum, the amounts of OH aliphatics and OH aromatics were inferred as 2.39 mmol g^{-1} and 0.44 mmol g^{-1}, respectively. This highlights the high content of OH aliphatics in the purified suberin. These OH aliphatics are found in the fatty alcohols and vicinal diols. Collectively, our data show that our isolated suberin retains a highly esterified arrangement due to the preservation of largely intact linear aliphatic esters combined with incomplete cleavage of acylglycerol esters. Based upon a comparison with the data obtained from our studies with cork, we believe that this is the closest to a native configuration of suberin reported to date.

We then isolated fractions of suberin through sequential collection of pellets formed at defined centrifugal forces, namely 96, 385, 865, 1538, and 2452 *g*. Nearly 98% of the total weight was recovered in the first three centrifuged fractions, accounting for 32.4, 50.4, and 15.0% w/w, respectively (Supplementary Fig. S12a). Their elemental composition displayed near identical signatures (Supplementary Table S1). Upon lyophilization, they showed similar ordered polygonal structures to those previously observed for suberin (Fig. 1b), but appeared to display distinct degrees of compactness (Fig. 4a). The denser fraction (96 *g*) is composed of more irregular shaped polygonal-*like* structures, most of which are highly condensed, but containing also a few porous open laced structures (Fig. 4a). When dissolved in DMSO, all of the fractions showed ^{1}H spectra that were virtually identical to that of suberin (Fig. 4b). This indicated little or no change in chemical composition between the samples. None of

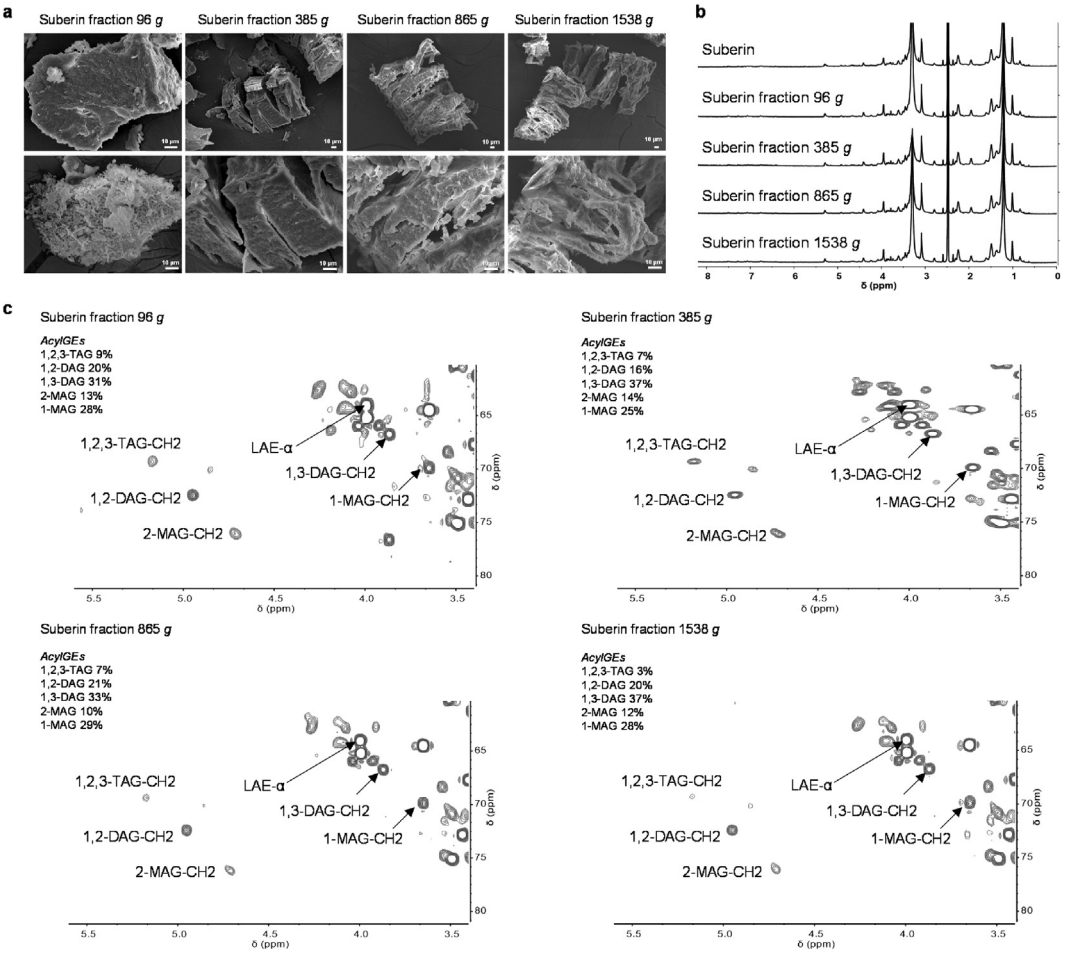

Fig. 4. Morphological and wide-ranging NMR spectral characterization of suberin centrifuged fractions. Suberin centrifuged fractions were obtained by sequential collection of pellets formed at defined centrifugation forces, namely 96, 385, 865, and 1538 *g* (plus a 2452 *g* minor fraction that accounts for less than 1% wt). (a) Their morphology was analyzed by SEM, (b–c) and their chemistry by wide-ranging NMR. (a) SEM imaging of the freeze-dried samples showed that they all formed ordered polygonal-*like* structures. (b) Their ^{1}H NMR spectra signatures were virtually identical, (c) but the glycerol CH-Acyl region of their corresponding HSQC-NMR spectra revealed extant differences in the relative abundance (%) of the distinct acylglycerol configurations. Text inserts in the HSQC spectra indicate the relative abundance (%) of the different acylglycerol configurations present within each sample as well as the ratio of aliphatic esters and acylglycerol esters. AcylGEs and LAEs stand for acylglycerol esters and linear aliphatic esters, respectively; TAG, DAG, and MAG stand for triacylglycerol, diacylglycerol, and monoacylglycerol, respectively.

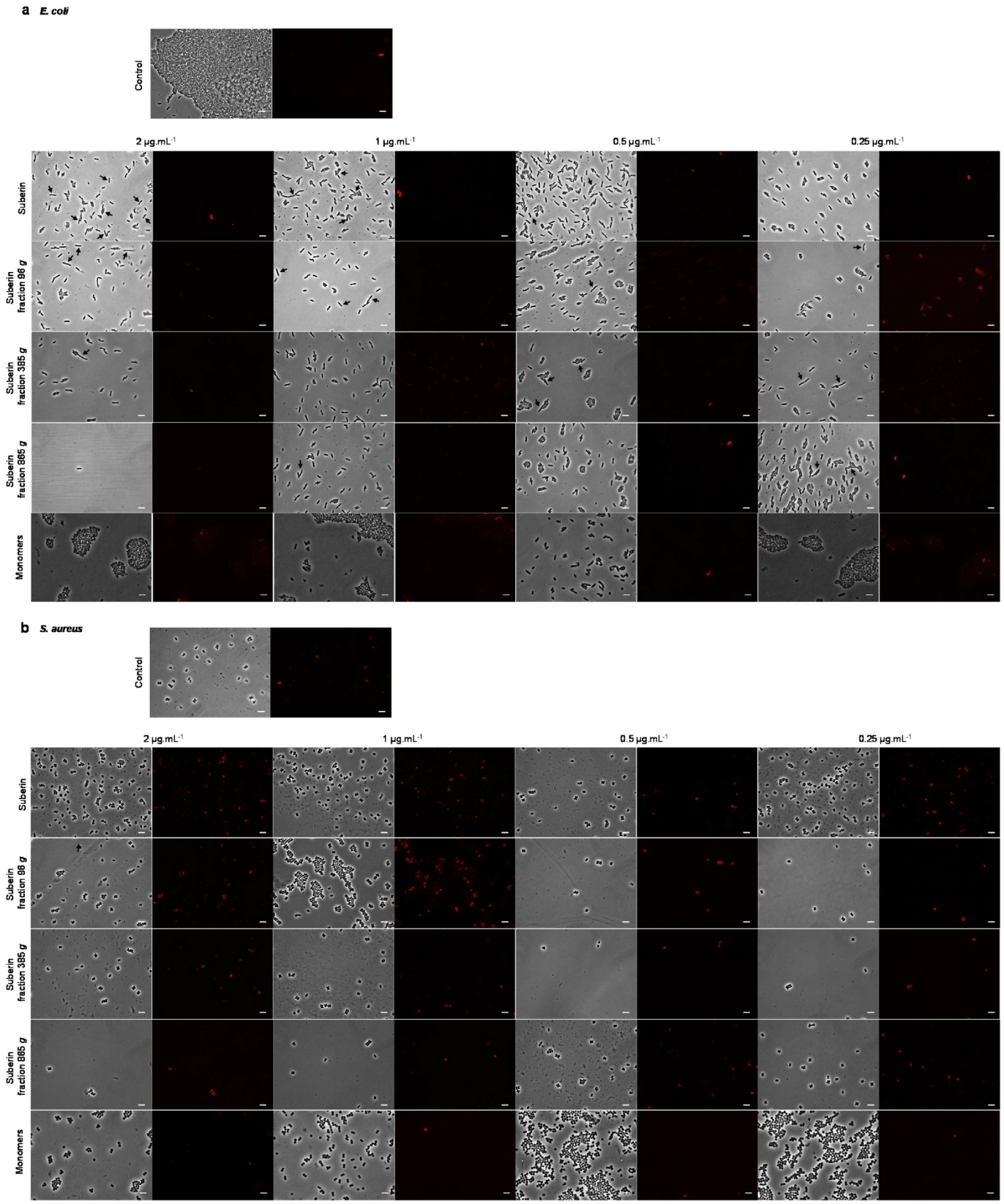

Fig. 5. Suberin activity against *E. coli* and *S. aureus*. Following exposure of (a) *E. coli* and (b) *S. aureus* cells to suberin at concentrations of 0.25–2 μg mL^{-1} (11 h), their morphology and viability were visualized by phase-contrast (arrows highlight the filamentous phenotype of *E. coli* cells, a) and fluorescence microscopy using Texas Red filter (dead cells show red fluorescence due to propidium iodide labeling, a–b), respectively. Controls are also shown (without suberin and a mixture of hydrolysate cork monomers). The scale bar in all images is 5 μm.

these samples were comprised of polymeric units that could be discriminated based on their self-diffusion coefficient as determined through DOSY-NMR (Supplementary Fig. S12b). This result is consistent with the thermal characterization of the fractions that revealed no major changes in molecular weight distributions or structural ordering when compared to suberin (Supplementary Fig. S1). Taken together, these observations suggest that the density differences of the centrifuged fractions are not due to molecular weight changes.

The centrifuged fractions were apparently 1.2-fold enriched in glycerol compared to the parental suberin sample (*ca.* 45 mg g^{-1} w/w) (Table 1). Their HSQC spectra revealed that 1,2,3-TAG was the least abundant acylglycerol configuration (Fig. 4c), as seen for the parental sample (Fig. 2e). The centrifuged fractions contained a higher relative abundance of DAG (16–30%) and a lower relative abundance of MAG (20%) compared to suberin (Fig. 4c). Between fractions, no great differences were noted, except that the least dense fraction (1538 *g*) contains less 1,2,3-TAG and more DAG compared with the more dense samples (Fig. 4c). There were differences ($p \leq 0.05$) in the specific amounts of hydrolyzable monomers (Table 1); however, none of the samples could be discriminated through principal component analysis (Supplementary Figure S13). The amounts of some particularly abundant suberin constituents (>5% wt), namely 9,10-dihydroxyoctadecanedioic acid, 24-hydroxytetracosanoic acid, and 9,10-epoxy-18-hydroxyoctadecanoic acid, decreased in the less dense samples, whereas octadecanedioic acid showed the opposite behavior. Note that only 9,10-dihydroxyoctadecanedioic acid and 24-hydroxytetracosanoic acid were found in higher amounts in the suberin sample.

Differences in monomeric composition and in the abundance and diversity of acylglycerol configurations will influence the supramolecular arrangement of the polymeric structures and possibly also their bioactivity. Preliminary evidence of suberin's bactericidal activity has been established using smooth materials solely manufactured with suberinic structures containing *ca.* 13% of the native glycerol [17]. Virtually all constituents of suberin, from fatty acids and their acylglycerides to aromatics, individually display the potential to affect cellular membrane functions in bacteria (*e.g.,* energy metabolism, fluidity, and permeability); an effect of fatty acids that is influenced by their chain lengths and appended functionalities [20,32]). *In planta,* suberin monomeric constituents are assembled into highly crosslinked and branched structural networks that have evolved for defensive roles. Herein, we observed that suberin, at a concentration of 500 μg mL^{-1}, formed aggregates on the microscale when placed in bacterial growth medium (size of *ca.* 1.3 ± 0.4 μm). These aggregates were able to kill *Staphylococcus aureus* and *Escherichia coli,* although they were more effective against *S. aureus* (data not shown). At concentrations of 0.25–2 μg mL^{-1}, we observed that suberin or its centrifuged fractions were dispersed as stable particles of 100–400 nm (with low dispersity; 0.52–0.93) during 24 h (Supplementary Table S5). Note that the large suberin aggregates observed by TEM imaging consisted of spherical structures of *ca.* 200–400 nm (Fig. 1). These showed notable similarity to polyhydroxy fatty acid nanoparticles known as cutinsomes (50–200 nm) [33], and these particles possibly constitute a suberinsome-*like* structure. We then evaluated the response of bacteria cells exposed for 11 h (exponential phase of growth) to either suberin or its centrifuged fractions, specifically looking at their cellular morphology and viability (Fig. 5). All samples were able to induce, to some extent, cell death in *S. aureus* and *E. coli* at the concentrations tested (Fig. 5a and b). The latter was less susceptible, but the presence of many elongated *E. coli* cells, the so-called filamentous phenotype, was observed (Fig. 5a). This filamentous phenotype is suggestive of major stress responses, *e.g.*, observed upon the treatment of cells with β-lactam antibiotics [34] or with some natural compounds with unknown cellular targets [35]. There were some differences between the antimicrobial activity of suberin and of its centrifuged fractions. The surface charge of all preparations (parental sample and centrifuged fractions) was near neutral (zeta potential ~0 mV; Supplementary Table S5). At this stage, it is not possible to associate a superior bactericidal activity with the observed enrichment in specific hydrolysate constituents (Table 1). The measured activity is certainly cumulative and is largely influenced by the supramolecular arrangement that is lost upon the hydrolysis used in the GC-MS analysis. This hypothesis is supported by the observation that the mixture of the cork hydrolysate monomers was largely unable to kill either bacterium (Fig. 5a and b). In addition, the observed differences between suberin and its fractions from which it is composed may also derive from changes in surface chemistry and/or topography. Notably, all suberin samples displayed bactericidal activity against important Gram+ and Gram- human pathogens (Fig. 5) in the range usually reported for antimicrobial peptides [32].

In summary, our methodological dissection of suberin structure has revealed an unexpected feature of this cryptic biopolymer: its ability to form suberinsome-*like* structures with bactericidal activity. Emphasis should be placed on the great degree of structural details revealed for suberin, both *ex situ* (purified) and *in situ* (in cork). The methodologies developed here now constitute essential tools for fingerprinting the multifunctionality of many complex biopolymers in order to better understand their structure and biological roles. Our methodological dissection of the suberin structure can be applied to many other heterogeneous biopolymers displaying high chemical and structural complexity and will lead to a better understanding of how to build complex polymer assemblies with added-value properties such as bactericidal activity.

Funding

We acknowledge funding from the European Research Council through grant ERC 2014-CoG-647928, from the European Union's Horizon 2020 research and innovation program within the project 713475 – FLIPT – H2020-FETOPEN-2014-2015 and from Fundação para a Ciência e Tecnologia (FCT) through the grant UID/Multi/04551/2019 (Research unit GREEN-it "Bioresources 4 Sustainability") and the project AAC 01/SAICT/2016 (CERMAX, ITQB-NOVA, Oeiras, Portugal). RR is grateful to FCT for the fellowship SFRH/BD/110467/2015. The authors would like to acknowledge the kind support in the framework of the COST Action EXIL – Exchange on Ionic Liquids (CM1206).

Authors' contributions

CSP supervised the project and the interpretation of data and prepared the final version of the manuscript. All authors have made substantial contributions to the acquisition, analysis, and interpretation of data and contributed to the drafting of the manuscript: VGC, JP, RR, and AB (ionic liquid synthesis and suberin extractions); VGC, AB, and AWTK (NMR data analysis); VGC and RR (suberin fractionation, microscopic and antimicrobial assays); JP, LH, and PS (GC-MS analyses); AB, MF, AG, and FV (thermal analyses); VGC (preparation of the initial draft of the manuscript). All authors read and approved the final version of the manuscript.

Declaration of competing interest

The authors declare no competing interests.

Acknowledgments

The authors acknowledge the use of equipment at the CERMAX NMR center (ITQB-NOVA, Oeiras, Portugal). The authors are extremely thankful to Pedro Lamosa and Maria C. Leitão (ITQB NOVA) for support in the NMR and chromatographic analyses, respectively, and to Mariana Pinho and Pedro Fernandes (ITQB NOVA) for help in the use of the fluorescence microscope. We also acknowledge S. Bonucci and E.M. Tranfield (IGC, Oeiras, Portugal) from the Electron Microscopy Facility at the Instituto Gulbenkian de Ciência for sample processing and technical expertise. The authors are also thankful to Celso Martins and James Yates

(ITQB NOVA) for support in statistical analyses and in English proof-reading of the manuscript, respectively.

Appendix A. Supplementary data

Supplementary data to this article can be found online at https://doi.org/10.1016/j.mtbio.2019.100039.

References

[1] B. Bakan, D. MArion, Assembly of the cutin polyester: from cells to extracellular cell walls, Plants 6 (2017) 57–68, https://doi.org/10.3390/plants6040057.

[2] E. Pineau, L. Kriegshauser, M. Schmitt, E.A. Fich, J.K.C. Rose, J. Ehlting, et al., A phenol-enriched cuticle is ancestral to lignin evolution in land plants, Nat. Commun. 8 (2017) 1–8, https://doi.org/10.1038/ncomms14713.

[3] P.E. Kolattukudy, Biopolyester membranes of plants: cutin and suberin, Science 208 (1980) 990–1000, https://doi.org/10.1126/science.208.4447.990.

[4] R. Franke, L. Schreiber, Suberin - a biopolyester forming apoplastic plant interfaces, Curr. Opin. Plant Biol. 10 (2007) 252–259, https://doi.org/10.1016/j.pbi.2007.04.004.

[5] L. Schreiber, Transport barriers made of cutin, suberin and associated waxes, Trends Plant Sci. 15 (2010) 546–553, https://doi.org/10.1016/j.tplants.2010.06.004.

[6] M. Pollard, F. Beisson, Y. Li, J.B. Ohlrogge, Building lipid barriers: biosynthesis of cutin and suberin, Trends Plant Sci. 13 (2008) 236–246, https://doi.org/10.1016/j.tplants.2008.03.003.

[7] H. Pereira, Chemical composition and variability of cork from Quercus suber L, Wood Sci. Technol. 22 (1988) 211–218, https://doi.org/10.1007/BF00386015.

[8] W. Wang, S. Tian, R.E. Stark, Isolation and identification of triglycerides and ester oligomers from partial degradation of potato suberin, J. Agric. Food Chem. 58 (2010) 1040–1045, https://doi.org/10.2217/FON.09.6.Dendritic.

[9] L. Moire, A. Schmutz, A. Buchala, B. Yan, R.E. Stark, U. Ryser, Glycerol is a suberin monomer. New experimental evidence for an old hypothesis, Plant Physiol. 119 (1999) 1137–1146, https://doi.org/10.1104/pp.119.3.1137.

[10] M.H. Lopes, A.M. Gil, A.J.D. Silvestre, C.P. Neto, Composition of suberin extracted upon gradual alkaline methanolysis of Quercus suber L. Cork, J. Agric. Food Chem. 48 (2000) 383–391, https://doi.org/10.1021/jf9909398.

[11] N. Cordeiro, M.N. Belgacem, A.J.D. Silvestre, C. Pascoal Neto, A. Gandini, Cork suberin as a new source of chemicals. 1. Isolation and chemical characterization of its composition, Int. J. Biol. Macromol. 22 (1998) 71–80, https://doi.org/10.1016/s0141-8130(97)00090-1.

[12] M. Petkovic, J.L. Ferguson, H.Q.N. Gunaratne, R. Ferreira, M.C. Leitão, K.R. Seddon, et al., Novel biocompatible cholinium-based ionic liquids—toxicity and biodegradability, Green Chem. 12 (2010) 643–649, https://doi.org/10.1039/b922247b.

[13] R. Ferreira, H. Garcia, A.F. Sousa, M. Petkovic, P. Lamosa, C.S.R. Freire, et al., Suberin isolation from cork using ionic liquids: characterisation of ensuing products, New J. Chem. 36 (2012) 2014–2024, https://doi.org/10.1039/c2nj40433h.

[14] H. Garcia, R. Ferreira, M. Petkovic, J.L. Ferguson, M.C. Leitão, H.Q.N. Gunaratne, et al., Dissolution of cork biopolymers in biocompatible ionic liquids, Green Chem. 12 (2010) 367–369, https://doi.org/10.1039/b922553f.

[15] R. Ferreira, H. Garcia, A.F. Sousa, C.S.R. Freire, A.J.D. Silvestre, L.P.N. Rebelo, et al., Isolation of suberin from birch outer bark and cork using ionic liquids: a new source of macromonomers, Ind. Crops Prod. 44 (2013) 520–527, https://doi.org/10.1016/j.indcrop.2012.10.002.

[16] R. Ferreira, H. Garcia, A.F. Sousa, M. Guerreiro, F.J.S. Duarte, C.S.R. Freire, et al., Unveiling the dual role of the cholinium hexanoate ionic liquid as solvent and catalyst in suberin depolymerisation, RSC Adv. 4 (2014) 2993–3002, https://doi.org/10.1039/C3RA45910A.

[17] H. Garcia, R. Ferreira, C. Martins, A.F. Sousa, C.S.R. Freire, A.J.D. Silvestre, et al., Ex situ reconstitution of the plant biopolyester suberin as a film, Biomacromolecules 15 (2014) 1806–1813, https://doi.org/10.1021/bm500201s.

[18] J. Graça, V. Cabral, S. Santos, P. Lamosa, O. Serra, M. Molinas, et al., Partial depolymerization of genetically modified potato tuber periderm reveals intermolecular linkages in suberin polyester, Phytochemistry 117 (2015) 209–219, https://doi.org/10.1016/j.phytochem.2015.06.010.

[19] C. Coquet, E. Bauza, G. Oberto, A. Berghi, A. Farnet, E. Ferré, et al., Quercus suber cork extract displays a tensor and smoothing effect on human skin: an in vivo study, Drugs Exp. Clin. Res. 31 (2005) 89–99.

[20] C.P. Churchward, R.G. Alany, L.A.S. Snyder, Alternative antimicrobials: the properties of fatty acids and monoglycerides, Crit. Rev. Microbiol. 44 (2018) 561–570, https://doi.org/10.1080/1040841X.2018.1467875.

[21] M. Emilia Rosa, H. Pereira, The effect of long term treatment at 100°C-150°C on structure, chemical composition and compression behaviour of cork, Holzforschung 48 (1994) 226–232, https://doi.org/10.1515/hfsg.1994.48.3.226.

[22] J. Graça, H. Pereira, Cork suberin: a glyceryl based polyester, Holzforschung 51 (1997) 225–234, https://doi.org/10.1515/hfsg.1997.51.3.225.

[23] S. Santos, V. Cabral, J. Graça, Cork suberin molecular structure: stereochemistry of the C18 epoxy and vic-diol ω-hydroxyacids and α,ω-diacids analyzed by nmr, J. Agric. Food Chem. 61 (2013) 7038–7047, https://doi.org/10.1021/jf400577k.

[24] S.M. Rocha, B.J. Goodfellow, I. Delgadillo, C.P. Neto, A.M. Gil, Enzymatic isolation and structural characterisation of polymeric suberin of cork from Quercus suber L, Int. J. Biol. Macromol. 28 (2001) 107–119, https://doi.org/10.1016/S0141-8130(00)00163-X.

[25] J.W. Emsley, J. Feeney, L.H. Sutcliffe, High Resolution Nuclear Magnetic Resonance Spectroscopy, Elsevier, 1966, https://doi.org/10.1016/S0076-695X(08)60516-5.

[26] H. Pereira, J. Graca, Methanolysis of bark suberins: analysis of glycerol and acid monomers, Phytochem. Anal. 11 (2000) 45–51, https://doi.org/10.1002/(SICI)1099-1565(200001/02)11:1<45::AID-PCA481>3.0.CO;2-8.

[27] S.D. Mansfield, H. Kim, F. Lu, J. Ralph, Whole plant cell wall characterization using solution-state 2D NMR, Nat. Protoc. 7 (2012) 1579–1589, https://doi.org/10.1038/nprot.2012.064.

[28] H. Kim, J. Ralph, Solution-state 2D NMR of ball-milled plant cell wall gels in DMSO-d6/pyridine-d5, Org. Biomol. Chem. 8 (2010) 576–591, https://doi.org/10.1039/b916070a.

[29] L. Kyllönen, A. Parviainen, S. Deb, M. Lawoko, M. Gorlov, I. Kilpeläinen, et al., On the solubility of wood in non-derivatising ionic liquids, Green Chem. 15 (2013) 2374–2378, https://doi.org/10.1039/c3gc41273c.

[30] A. Björkman, Isolation of lignin from finely divided wood with neutral solvents, Nature 174 (1954) 1057–1058, https://doi.org/10.1038/1741057a0.

[31] A.V. Marques, A. Gutiérrez, J. Rencoret, H. Pereira, J.C. del Río, Ferulates and lignin structural composition in cork, Holzforschung 70 (2015) 275–289, https://doi.org/10.1515/hf-2015-0014.

[32] A.P. Desbois, V.J. Smith, Antibacterial free fatty acids: activities, mechanisms of action and biotechnological potential, Appl. Microbiol. Biotechnol. 85 (2010) 1629–1642, https://doi.org/10.1007/s00253-009-2355-3.

[33] J.A. Heredia-Guerrero, M.A. San-Miguel, M. Luna, E. Domínguez, A. Heredia, J.J. Benítez, Structure and support induced structure disruption of soft nanoparticles obtained from hydroxylated fatty acids, Soft Matter 7 (2011) 4357–4363, https://doi.org/10.1039/c0sm01545h.

[34] C. Chalut, X. Charpentier, M.H. Remy, J.M. Masson, Differential responses of Escherichia coli cells expressing cytoplasmic domain mutants of penicillin-binding protein 1b after impairment of penicillin-binding proteins 1a and 3, J. Bacteriol. 183 (2001) 200–206, https://doi.org/10.1128/JB.183.1.200-206.2001.

[35] S. Derakhshan, M. Sattari, M. Bigdeli, Effect of subinhibitory concentrations of cumin (Cuminum cyminum L.) seed essential oil and alcoholic extract on the morphology, capsule expression and urease activity of Klebsiella pneumoniae, Int. J. Antimicrob. Agents 32 (2008) 432–436, https://doi.org/10.1016/j.ijantimicag.2008.05.009.